NORTHWESTERN UNIVERSITY

Reconstructions on Strontium Titanate (110) Surfaces at Various Annealing Conditions

A THESIS

SUBMITTED TO THE GRADUATE SCHOOL
IN PARTIAL FULFILLMENT OF THE REQUIREMENTS

for the degree

MASTER OF SCIENCE

Field of Materials Science and Engineering

by

Alicia Loon

EVANTON, ILLINOIS

August 2011

Abstract

Reconstructions on Strontium Titanate (110) Surfaces at Various Annealing Conditions

Alicia Loon

Strontium titanate (SrTiO$_3$) is a perovskite complex metal oxide used in many different applications due to its tunable multifunctional properties. Understanding the surface dynamics of strontium titanate is crucial for the engineering and design of functional structures. Research on the polar SrTiO$_3$ (110) remains relatively scarce and findings from different groups vary greatly. Several (nx1) reconstructions in which the reconstruction type depends on sample preparation and treatment conditions were observed. In this study, reconstructions on air-annealed SrTiO$_3$ (110) were examined using transmission electron diffraction and microscopy. It was observed that samples annealed in air between 875°C and 1050°C for 5 hours reconstructed with a (1x5) type reconstruction. At 1150°C, the sample showed (1x4) and (1x5) reconstructions after 3 hours, but displayed a (5x1) periodicity instead after 5 hours. Annealing at 1250°C for 5 hours resulted in a fully reconstructed (5x1) periodicity. Measured electron diffraction amplitudes of the (1x5) reconstruction coupled with direct method analysis provided reasonable initial estimates of the true surface structure. Peaks refinement and density functional theory calculations narrowed down the possible solution set to several structures that seem highly possible. Currently there is a model that matches all known constraints but no conclusive results have been reached. More ongoing work is being done to solve the structure.

Acknowledgments

First of all, I would like to express my gratitude to my research advisor, Professor Laurence D. Marks, for his guidance, assistance and encouragement. This research project would not have been possible without the education and insights he provided.

I would like to thank my undergraduate research mentor, Dr. James A. Enterkin, who taught me the basics of all experimental procedures and stayed past office hours to assist me in many TEM sessions. I would also like to acknowledge Danielle M. Kienzle, a Ph.D. candidate in this group, for her guidance in using EDM, ATOMS, CRYSCON and other programs used in this research. I am grateful to all past and present members in the Marks Group, who shared with me many tips and tricks in both the experimental and computational work of this research project, making my research and education experience more pleasant.

I am also thankful to Dr. Kathleen A. Stair. Her guidance and advice on writing a good undergraduate thesis have helped me a lot in preparing this Master's Thesis. I would like to thank staff members in the NUANCE Center at Northwestern University, Dr. Jinsong Wu and Dr. Shuyou Li, who assisted with my experimental work in the EPIC facility.

Last but not least, I would like to extend my deepest gratitude to my family and friends who accompanied me through thick and thin all these years. Without their continued support and encouragement, I would not have been able to make it this far. Thank you for having faith in me.

Contents

List of Tables

List of Figures

Chapter 1

Introduction

1.1 Why Surface Science?

Understanding and characterizing surfaces at the atomic scale is increasingly important nowadays as science and technology in various disciplines move toward the nano- and pico-scales. Surface and interfacial properties become more important relative to bulk properties as technologies develop on materials at smaller length scales. Unlike bulk atoms, surface atoms suffer a loss of coordination. The undercoordinated bonds increase the surface free energy, providing a driving force for the surface atoms to reconstruct to achieve a more stable, lower energy state. Besides, surface atoms also interact with their immediate surroundings and may react chemically with their neighboring materials. Structural and compositional changes at the surface give rise to unique physical and chemical properties different from those of the bulk (Klauber et al., 2003). In fact, bulk characterization techniques that were used prior to the advent of surface science in the 1970's failed in diagnosing why some surface catalysts deactivated or died prematurely (Bhasin, 1999). Catalysts sharing the same bulk composition have different surface structures that cannot be adequately characterized using bulk characterization techniques. Since there was no way to differentiate these seemingly same catalysts that performed differently, scientists and engineers used to regard catalysis as an "art" or "magic" (Bhasin, 1999). Surface science studies have greatly improved the understanding of many catalysis systems, and are crucial to the discovery and development of better catalysis processes for industrial and commercial applications (Bhasin, 1999).

Since the structure of reconstructed surfaces cannot be predicted *a priori* using bulk thermodynamic arguments, the surface atomic structure of materials needs to be determined experimentally (Chiaramonti, 2005). There are various techniques to experimentally study the atomic structure of surfaces. Some of the common techniques used in real space surface studies include scanning tunneling microscopy (STM), atomic force microscopy (AFM), transmission electron microscopy (TEM), high-resolution electron microscopy (HREM) and scanning transmission electron microscopy (STEM). Surface studies in reciprocal space often use techniques such as low-energy electron diffraction (LEED), transmission electron diffraction (TED), and reflection high-energy electron diffraction (RHEED). Spectroscopic techniques such as X-ray photoelectron spectroscopy (XPS) and Auger Electron Spectroscopy (AES) were also used to detect chemical composition and electronic structure of surfaces. Advantages and limitations of many of the above-mentioned techniques as well as their applications to surface crystallography have been reviewed by Venables et al. (1987) and Subramanian and Marks (2004). Of the aforementioned surface characterization techniques, transmission electron microscopy methods including TEM, TED and HREM are able to capture from the same area in the specimen both real and reciprocal space information. In this study, TEM techniques and electron direct methods (EDM) together with complimentary techniques such as STM were used to study the surface reconstructions of strontium titanate (110) upon annealing.

1.2 Why Strontium Titanate?

Strontium titanate ($SrTiO_3$) is a prototypical perovskite, a class of materials with ABO_3 stoichiometry, where the A-site cation is typically either an alkaline or alkaline earth metal whereas the B-site cation is typically a first-row transition metal. The bulk structure of the

perovskite $SrTiO_3$ consists of a simple cubic with the strontium at the cube vertices, titanium at the body center and oxygen at the face centers (Figure 1.1).

Perovskites are fascinating in that many properties of these materials can be easily tuned by varying the A- or B-site cations, or the oxygen content (Attfield, 2001). Strontium titanate, for example, has intrinsic properties that can be tuned by various levels of doping. It has been shown that subtle changes at the surface can functionalize strontium titanate surfaces to be highly conductive or blue-light emitting (Deak, 2007). Strontium titanate single crystals have demonstrated ultraviolet photosensitive properties, making them potentially useful in environmental monitoring applications such as ozone hole sensing and fire detection (Huang et al., 2007). Having a lattice parameter of 3.905Å at room temperature, strontium titanate also interfaces well with other perovskites by offering minimum lattice mismatch (Biswas et al., 2011). Some of these interfaces display interesting and sometimes unexpected phenomena, which are well-documented in the literature (Copie et al., 2009; Huijben et al., 2009). A thorough understanding of strontium titanate surfaces is thus important for these surfaces to find their way into a wider scope of applications.
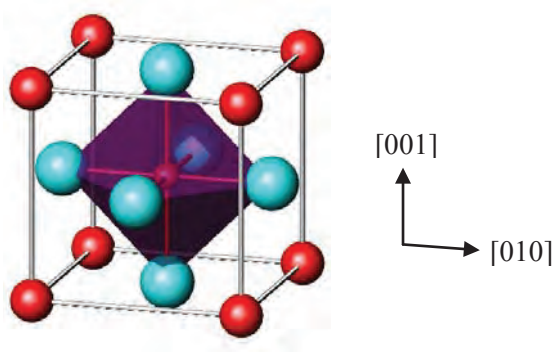
Figure 1.1. Bulk structure of the perovskite $SrTiO_3$ consisting a simple cubic lattice of strontium with titanium at the body center and oxygen at the face centers. The titanium octahedron is shown.

Among the low-index strontium titanate surfaces, strontium titanate (001) has been studied in various theoretical and experimental work that covered a wide range of treatment conditions. Several reconstruction types have been solved (Castell, 2002; Erdman et al., 2002; Deak, 2007). There are comparatively fewer studies focusing on the (111) surfaces and the structure has not been solved although many different reconstructions have been observed depending on sample preparation and annealing conditions (Chiaramonti et al., 2008; Marks et al., 2009). Very limited experimental work has been done on the (110) surfaces and only one reconstruction type has been solved to date (Enterkin et al., 2010). The current work thus focuses on the (110) surfaces to further characterize the lesser-known surface.

Strontium titanate (110) is a polar surface consisting of alternately-stacked $SrTiO^{4+}$ and O_2^{4-} layers (Figure 1.2). Based on classical electrostatic arguments, these layers that have equal but opposite charges give rise to a non-zero dipole moment normal to the surface in all repeating units of the material along [110], causing the (110) surface to have a diverging electrostatic surface energy and become unstable. Since bulk truncation is energetically unfavorable, the surface has to undergo one or more mechanisms to stabilize the macroscopic dipole moment and achieve a more stable, lower energy state. These mechanisms may include surface relaxation, covalency changes at the surface, modification of surface electronic structure, and changes in surface stoichiometry. Modification of surface electronic structure or stoichiometry by means of microfacetting, desorption of atoms, and reconstruction can neutralize the dipole (Noguera, 2000). According to Russell and Castell (2008), there could be more than one stoichiometry that can form stable surface phases, therefore it is possible to have several reconstruction types coexisting on the crystal surface.
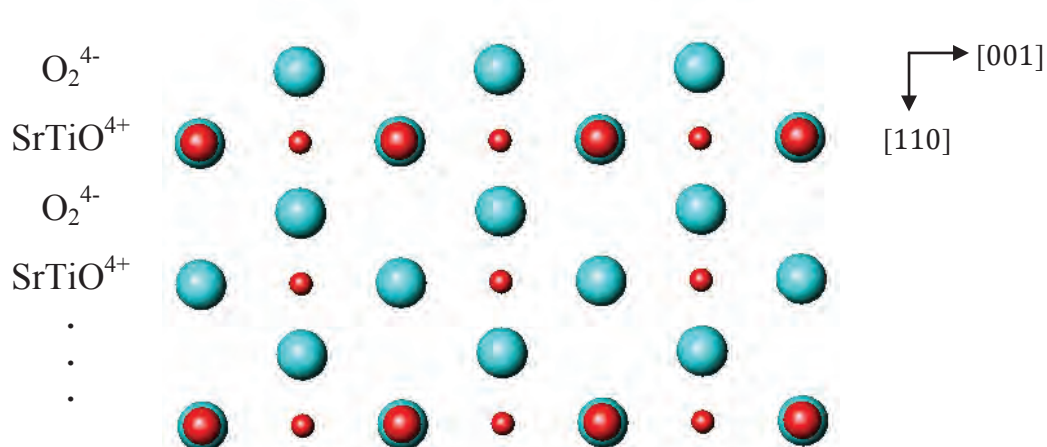
Figure 1.2. Alternately-stacked $(SrTiO)^{4+}$ and $(O_2)^{4-}$ layers along the [110] direction of $SrTiO_3$.

1.3 What is surface reconstruction?

As mentioned in the previous section, strontium titanate (110) has to neutralize the dipole to achieve a lower energy state and surface reconstruction is one of the mechanisms to do so. Under appropriate environmental conditions, surface atoms will rearrange themselves into periodicities larger than the bulk periodicity by displacing some surface atoms. This is known as surface reconstruction (Lanier, 2007). Surface reconstructions are commonly defined in Wood's notation, which is well-documented in the literature (Oura et al., 2003). In the case of $SrTiO_3(110)$, the first digit represents reconstruction in the [001] direction and the second the [1$\bar{1}$0] direction (Russell and Castell, 2008). For example, a (3x1) reconstruction means the reconstruction along the [001] direction is three times the (1x1) periodicity of the bulk whereas a (1x3) reconstruction indicates the [1$\bar{1}$0] direction shows a reconstruction that is three times the (1x1) bulk unit cell (Figure 1.3).
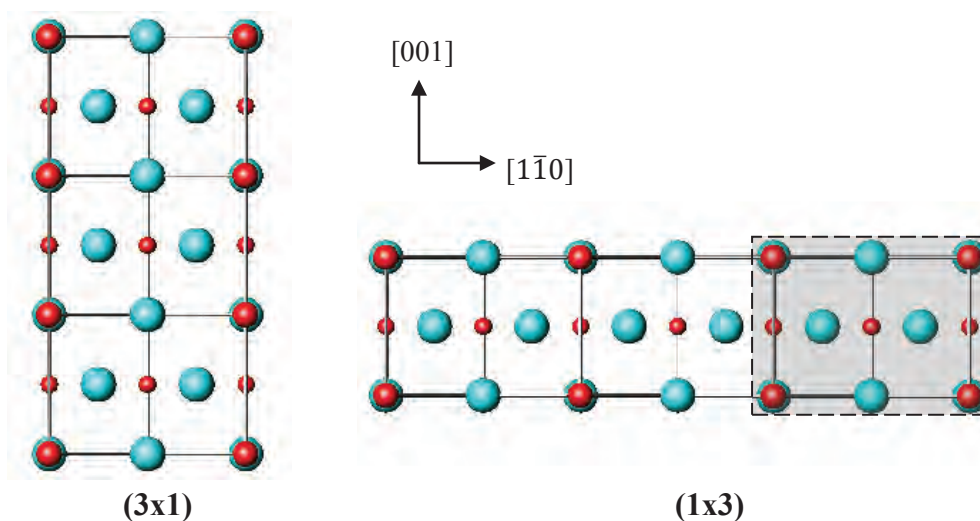
Figure 1.3. Different reconstruction types indicated using the Wood's notation. The grey square shows the (1x1) bulk periodicity.

The type of surface reconstruction is dictated by the environmental conditions the surface is exposed to. Gas composition and pressure, annealing time and temperature, presence of foreign elements and so on will affect how surface atoms rearrange themselves (Lanier, 2007; Marks et al., 2009). Sample preparation method could also affect reconstruction type. It was observed that two separate strontium titanate TEM specimen annealed in the same alumina combustion boat and having identical annealing conditions displayed different reconstruction types. It is predicted that parameters in ion milling such as ion energy and milling time might have an effect on surface reconstruction (Enterkin, 2009).

There is an enormous number of variables that affect surface reconstruction types. If these variables are known and carefully controlled, they may enable the engineering and design of functional surface structures. The motivation of the current work is to investigate how varying annealing temperature and time affect the surface reconstructions on strontium titanate (110).

Chapter 2

Experimental Procedures and Techniques

2.1 Characterization Techniques

Characterization techniques used in previous work on $SrTiO_3$ (110) include scanning tunneling microscopy (STM), low energy electron diffraction (LEED), Auger electron microscopy (AES), atomic probe microscope (AFM), X-ray photoemission spectroscopy (XPS), Raman spectroscopy, transmission electron microscopy (TEM) etc. Theoretical studies including density functional theories (DFT) and hybrid classical-quantum methodologies are important in characterizing the surface (Deak, 2007).

In this study, transmission electron microscopy (TEM) techniques were employed with transmission electron diffraction (TED) being the primary method. Electron diffraction via the TEM is a powerful method for characterizing surface structures. Many new structures were discovered or characterized in the past using TED, either alone or combined with other diffraction methods (Bendersky and Gayle, 2001). Transmission electron microscopy allows the observation of images and diffraction patterns from the same area of the specimen. The ability to collect real and reciprocal space information is a great advantage of TEM. Another major advantage of using TED in crystallographic studies is that the electron beam can be focused to very fine probe sizes, making TED highly sensitive to small deviations from an average structure. Small changes in the structure due to ordering, distortion, or presence of defects will result in observations of weak superstructure reflections or diffuse intensity (Bendersky and Gayle, 2001). The weak superstructure spots can be readily measured to determine surface periodicities, which

are different from the bulk periodicity. Coupled with post-processing routines, transmission electron diffraction data could provide important structural information necessary to solve a structure (Subramanian and Marks, 2004). Crystallographic direct methods, for instance, can be applied to generate potential maps from measured diffracted beam amplitudes, providing good estimates for structure refinement. This will be discussed in further detail in the next sections.

2.2 Sample Preparation

High purity single crystal $SrTiO_3$(110) wafers purchased from MTI Corporation were prepared using the standard TEM sample preparation method, annealed at various conditions, and examined using TEM to obtain electron diffraction patterns.

First, the $SrTiO_3$ (110) wafers measuring $10x10x0.5mm^3$ were cut into discs measuring 3mm in diameter using a circular disc cutter. The discs were thinned down to approximately 100μm by mechanical polishing using SiC paper. A Nikon optical microscope was used to determine the thickness by noting the difference in focus position (Brasunas et al., 1999). The discs were then dimpled on one side using a Gatan Dimple Grinder until the center of the sample was approximately 20μm. The sample was then ion milled using a Gatan Precision Ion Polishing System (PIPS) with 3-6kV argon ion beam at 3-5 degrees from the sample surface until a tiny hole or Newton rings was observed under the optical microscope. Each sample was annealed in air at different times and temperatures using a high temperature tubular furnace. A clean quartz tube with both ends open to anneal the sample in air was inserted into the tubular furnace. The sample was carefully put into an alumina combustion boat, which was then inserted into the quartz tube. The temperature was set to ramp up at a rate of 5°C per minute to the desired maximum temperature, dwell for a desired number of hours, and ramp down at a rate of 5°C per

minute to room temperature. The annealing temperature range of 875-1250°C used in this study was chosen based on similar parameters used in previous work. Heat treatment parameters for each anneal in this study are tabulated in Table 2.1. The annealed samples were then examined using the transmission electron microscope.

Table 2.1 Annealing temperature and time for each individual sample

Sample	1	2	3	4	5	1b*	2b*	6	7
Temperature (°C)	875	950	1050	1150	1250	875	950	1150	1150
Time (hours)	5	5	5	5	5	15	15	1	3

*Note: After being viewed under the microscope, samples 1 and 2 were annealed for an additional 10 hours and reused as samples 1b and 2b.

2.3 Transmission Electron Microscopy

The annealed $SrTiO_3$ (110) samples were viewed under the Hitachi H-8100 TEM and electron diffraction patterns from a thin specimen region were recorded. Since fine probe sizes make TED sensitive to changes in surface structures (Bendersky and Gayle, 2001), the smallest condenser lens aperture and the smallest spot size was used to obtain good diffraction data. When recording electron diffraction, the sample was tilted slightly off the zone axis to obtain a more kinematical diffraction condition and reduce dynamical diffraction effects. At the zone axis, there are plasmon scattering around the bulk spots and dynamical scattering by the bulk materials (Subramanian and Marks, 2004). Tilting slightly off the zone axis is akin to using precession electron diffraction techniques (Marks, 2011), which give intensities strikingly similar to kinematical amplitudes (Own, 2005). The specimen was also tilted such that the beam intensities on both sides of the transmitted beam decay as symmetrically as possible along the Laue circle. Practicing the above-mentioned techniques, one can obtain approximately kinematical diffraction.

Kinematical approximation can thus be applied and structural completion using direct methods can be attempted (Subramanian and Marks, 2004).

Standard TEM diffraction contrast imaging modes, Bright Field (BF) and Dark Field (DF), were used to study surface morphologies, such as faceting and terraces, on the area from which diffraction patterns were taken. Although they are low-resolution modes, BF and DF can be used to detect dislocations, voids, and bending in the sample.

Due to the nature of this project (to solve the structure using TED) and time constraints, high-resolution images (HREM) were not taken over the course of experimentation. High-resolution plan-view imaging would give images with low signal levels and may cause radiation damage. Beam damage may occur too quickly before HREM analysis could be performed, as mentioned in the work of Chiaramonti et al. (2008). Regardless of whether the HREM images were taken with the sample on-zone or tilted off-zone, image processing would be required to remove bulk spots that dominate the lattice contrast (Subramanian and Marks, 2004). There are numerous image processing techniques that allow more information to be extracted from HREM images (Marks, 1996). For more information regarding HREM in surface reconstruction studies, please refer to the work of Subramanian and Marks (2004), and Erdman et al. (2002).

2.4 Electron Direct Methods

Compared to reciprocal space information, real space imaging techniques have limited resolution due to the weak signals from only a few atomic layers, and are often insufficient to solve a structure. Intensities of diffraction beams, on the other hand, can be easily measured with precision and the resolution is superior. Diffraction experiments, however, only provide information on the amplitude (square root of the measured intensities). The phases of the

diffracted beams are lost. Both the phases and the amplitude are needed to obtain the complete structure factor. If both phases and amplitude were known, a simple Fourier inversion would give a scattering potential map, revealing the surface structure. Fortunately, there are various structure determining techniques that can provide an estimate reasonably close to the true surface structure, making structure refinement much easier. These techniques are collectively known as crystallographic direct methods (Subramanian and Marks, 2004; Marks et al., 2001).

A detailed explanation of Electron Direct Methods (EDM) is beyond the scope of this work, but an overview is provided below to illustrate the important role EDM plays in solving a structure. The basic idea of crystallographic direct methods is using *a priori* information as constraints to reduce possible phase values to a manageable number for structure refinement work. Common constraints include atomicity (scattering comes from atoms thus the solution should have atomistic features), positivity (charge density of the crystal must be positive) and localization (only near-surface atoms can be significantly displaced from bulk positions) (Subramanian and Marks, 2004). Using these constraints, phases of measured reflections from TED can be refined iteratively to find a small set of solutions used as starting points for approximating atomic locations. For more rigorous derivation and detailed explanation, please refer to Marks et al. (2001).

Electron Direct Methods have been used to solve many structures. In the case of $SrTiO_3(110)$, EDM is powerful in identifying only part of the structure since only a limited number of diffraction beams in the entire set were measured and among those, only surface spots that do not overlap with bulk spots can be measured. Complementary techniques such as Fourier-difference and projection-based methods within the Peaks2D refinement code further refine the structure determined from EDM (Chiaramonti, 2005).

Chapter 3

Reconstructions on Strontium Titanate (110) Surfaces
at Various Annealing Conditions

3.1 Previous Work

Although there is a seemingly large number of studies on $SrTiO_3$ (110), only a limited amount of experimental work has been done on $SrTiO_3$ (110). Many theoretical studies proposed structures derived from bulk terminations and these structures do not match experimentally observed unit cells (Enterkin et al., 2010). Some of the more recent experimental studies relevant to the current work are summarized below.

Bando et al. (1995) observed using STM step edges along $[1\bar{1}0]$ and a (5x2) reconstruction after annealing at 800°C for 3 hours. After 1100-1200°C annealing, ordering along [001] was more dominant and reconstructions of (4x2) or (5x2) type were observed. Using low energy electron diffraction (LEED), Brunen and Zegenhagen (1997) found different surface reconstructions of type (nxm) on $SrTiO_3$ (110) annealed at different conditions. $SrTiO_3$ (110) samples were annealed for 2-20 hours at 900-1100°C in ultra-high vacuum (UHV) with a heating and cooling rate of 30°C/min. The observation of (2x5), (3x4), (6x6), and (4x4) reconstructions were supported by scanning tunneling microscopy (STM) measurements. It was found that annealed samples display domains of different reconstructions. Samples that were sputtered before the annealing treatments have a more homogeneous surface structure. Missing spots were seen in the LEED patterns of all samples. STM images at that time did not provide sufficient atomic details, hence a later study by Russell and Castell (2008) suggested that the observed (3x4) reconstruction could be interpreted as a (3x1)/(1x4) coreconstruction on the sample surface.

Other than (nxm) type reconstructions, microfaceting was also observed on STO (110) surfaces. Gunhold et al. (2004) found that a sample annealed at 900°C in 1 atm air and another at 1000°C in UHV both showed faceting with (1x1) and (1x2) periodicity. This observation was supported by AES measurements. It was found experimentally that annealing samples in air at temperatures above 1000°C produced atomically flat STO (110) surfaces. After being annealed at 1000-1100°C under appropriate annealing conditions, sample surfaces with disordered step edges recrystallized and transformed morphologically to faceted step edges. Faceting of step edges occurred along several closely packed oxygen directions and the strongest faceting was observed along the $[1\bar{1}0]$ and $[001]$ directions (Bachelet et al., 2007).

In 2008, Russell and Castell observed (3x1) reconstruction in a sample annealed in UHV at 875°C for 2 hours. Annealing at 1100°C for 2 hours produced a sample showing (4x1) reconstruction. Another sample annealed at 1275°C showed (6x1) reconstruction. The (3x1) reconstructed surface contained (1x4) reconstruction at the step edges. Similarly, the (6x1) reconstruction showed (1x2) reconstruction on the lower terrace at the step edges, though the (1x2) on (6x1) reconstruction was not as common as the (1x4) on (3x1).

Using transmission electron diffraction and direct methods, Enterkin et al. (2010) solved the (3x1) reconstruction, which was found to have rings of TiO_4 tetrahedra. Varying the number of TiO_4 tetrahedra per ring forms a homologous series of (nx1) reconstructions. The results were confirmed through density functional theory (DFT) calculations and the structures agree with STM images obtained by Russell and Castell (2008) although sample preparation and heat treatments in this study (annealed at 1000°C under flowing O_2) were slightly different from those in Russell and Castell (2008). This study demonstrated that the bond-valence sums method

widely known in inorganic chemistry was found to be applicable in predicting oxide surface structures.

Reconstructions observed in previous studies together with their respective annealing conditions were summarized in Table 3.1. Most of the previous work involved annealing under UHV conditions at shorter times (1-3 hours) although some samples were reported to have been preheated to remove initial contamination. More work has to be done to examine reconstruction types on $SrTiO_3$ (110) surface under different annealing conditions. The current work aims to use transmission electron diffraction to investigate surface reconstructions of $SrTiO_3$ (110) annealed in ambient air.

Table 3.1. Summary of observed reconstructions on $SrTiO_3$ (110) surfaces in previous work.

Temperature (°C)	Time (hours)	Environment	Reconstructions	Analysis	Group
800	3	UHV	(5x2)	STM	Bando et al.
1100-1200	3	UHV	(4x2) or (5x2)		
960	2	O₂	(2x5)	LEED	Brunen and Zegenhagen
960	20	O₂	(4x4)		
*900; 910	4; 2	O₂	(3x4)		
900	1	Synthetic air (20% O₂, 80% N₂)	(1x1) and (1x2)	STM, AFM, AES	Gunhold et al.
1000	1	UHV	(1x1)		
875	2	UHV	(3x1) and (1x4)	STM, LEED	Russell and Castell
1100	2	UHV	(4x1)		
1275	2	UHV	(6x1) and (1x2)		
1100	N/A	O₂	(3x4)		Subramanian

*Note: This sample was first annealed at 900°C for 4 hours then annealed again at 910°C for 2 hours.

3.2 Dark Field Images

      All dark field images of samples annealed for 5 hours showed terraces of varying sizes (Figure 3.1). The bright and dark thickness fringes appear to be quantized within a given fringe, and would look more continuous at a lower magnification (Figure 3.1a). Each terrace is of uniform thickness, hence wide terraces indicate the sample is relatively flat. White dots were observed on the 950°C, 1150°C, and 1250°C anneals. These defects could be either voids in the sample or contaminants. The white spots were not observed on the 1050°C anneal, possibly because the image contrast was too low for them to be clearly visible.

      For the 950°C anneal (Figure 3.1b), the thickness fringes looked disordered, suggesting that the surface has not yet fully reconstructed to form orderly step edges. For the 1050°C anneal (Figure 3.1c), the terraces appeared in a tile-like manner, suggesting a surface more ordered than that of the 950°C anneal. The 1150°C anneal (Figure 3.1d) showed discrete bright and dark bands with width varying from approximately 50-80nm. These straight fringes suggest the presence of fairly uniform step edges or terraces. The 1250°C anneal (Figure 3.1e) did not show straight bands similar to those observed in the 1150°C anneal, but each terrace region was wider (measuring approximately 60-200nm) than those observed in lower temperature anneals.

      The size of the terraces increases with increasing annealing temperature. This suggests that the surface structure that was disordered after ion milling restored itself to be more ordered at higher temperatures.

      Faint streaks that could indicate surface reconstructions were observed in some of the DF images, such as Figure 3.1b. Using the software DigitalMicrograph[TM], Wiener filtering was applied to the image (Figure 3.2a) to reduce background noise and to make the streaks more visible (Marks, 2011). Line profiles of regions in the image that showed streaking were obtained
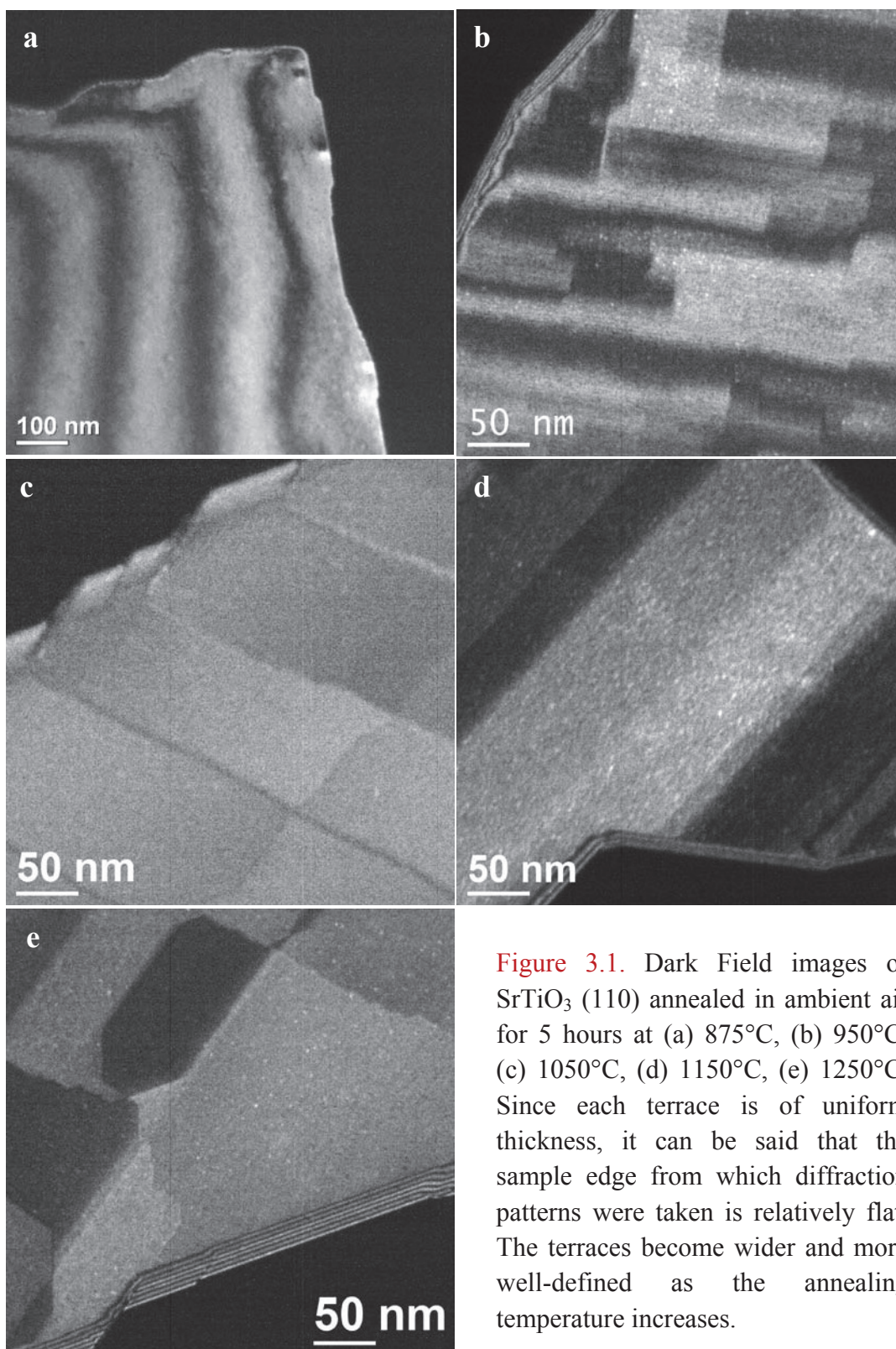
Figure 3.1. Dark Field images of SrTiO$_3$ (110) annealed in ambient air for 5 hours at (a) 875°C, (b) 950°C, (c) 1050°C, (d) 1150°C, (e) 1250°C. Since each terrace is of uniform thickness, it can be said that the sample edge from which diffraction patterns were taken is relatively flat. The terraces become wider and more well-defined as the annealing temperature increases.

using the line profile tool in the software. The varying intensity counts in each line profile (Figure 3.2b) indicate alternating bright and dark stripes in the image. Since image contrast in DF images corresponds to thickness of the specimen, the bright and dark stripes also indicate different heights of the surface structure. Measuring the distance between intensity peaks, the spacing between regions of similar height was obtained (Figure 3.2c). The average measurements of these spacings are close to the length of 5 times the (1x1) unit cell in the $[1\bar{1}0]$ direction, indicating a (1x5) reconstruction.

(a)
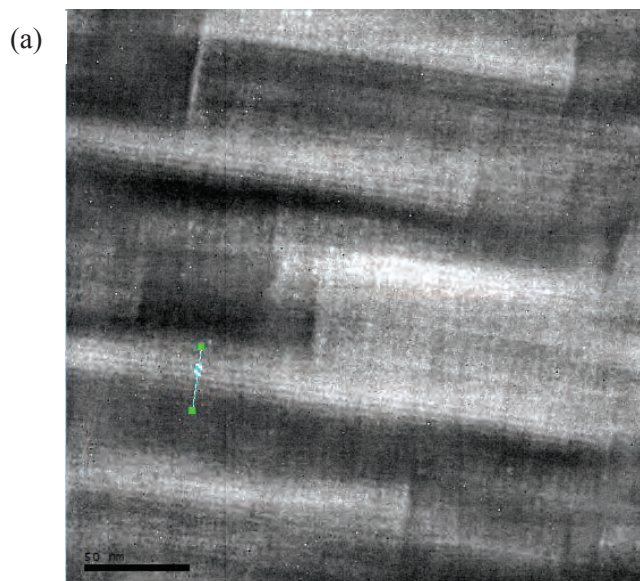
Figure 3.2.

(a) A Wiener-filtered DF image showing streaking, which indicates reconstruction. (b) A line profile was obtained to measure spacings between the streaks. (c) The averaged measured spacings are close to 5 times the (1x1) unit cell spacing in the $[1\bar{1}0]$ direction, indicating a (1x5) reconstruction.

(b)

(c)
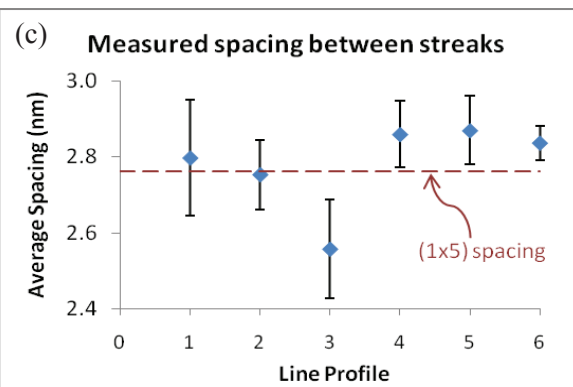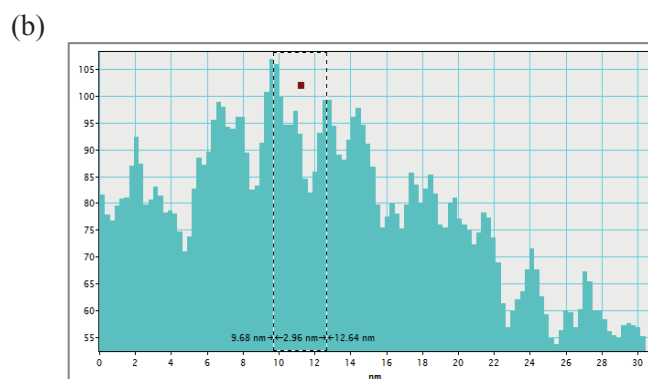
3.3 Transmission Electron Diffraction

Using transmission electron diffraction (TED), (nx1) reconstructions (n = 4 or 5) were found in samples air-annealed at higher temperatures for a longer period of time. This agrees with experimental data found in the literature. However, (1xn) periodicities were observed as the dominant reconstruction type in samples air-annealed at lower temperatures. In previous work, (1xn) was found only at the step edges, coexisting with more dominant (nx1) reconstructions (Russell and Castell, 2008).

Based on the TED data, annealing $SrTiO_3$ (110) at 1250°C for 5 hours resulted in a (5x1) reconstruction (Figure 3.3a). At 1150°C, the same reconstruction was observed although there is slight streaking in the [1$\bar{1}$0] direction. However, after annealing for only 3 hours at 1150°C, (1x5) and (1x4) reconstructions were found to coexist (Figure 3.3b). This suggests that there might be a change in reconstruction type at this time and temperature range. In the 1050°C anneal, four weak diffraction spots from the surface atoms were observed to be fairly evenly spaced between two bulk diffraction spots along the [1$\bar{1}$0] direction, indicating a fully reconstructed (1x5) surface (Figure 3.3c). The 875°C and 950°C anneals show streaking along the [1$\bar{1}$0] direction (Figure 3.3d), although the diffraction spots were more discrete in the 950°C anneal, suggesting the surface had reconstructed more fully.

The 875°C and 950°C anneals were subjected to an additional 10 hours of annealing time. The samples had not fully reconstructed when annealed for only 5 hours, but after a total annealing time of 15 hours, evenly spaced surface diffraction spots were observed in the [1$\bar{1}$0] direction, indicating a (1xn) reconstruction.
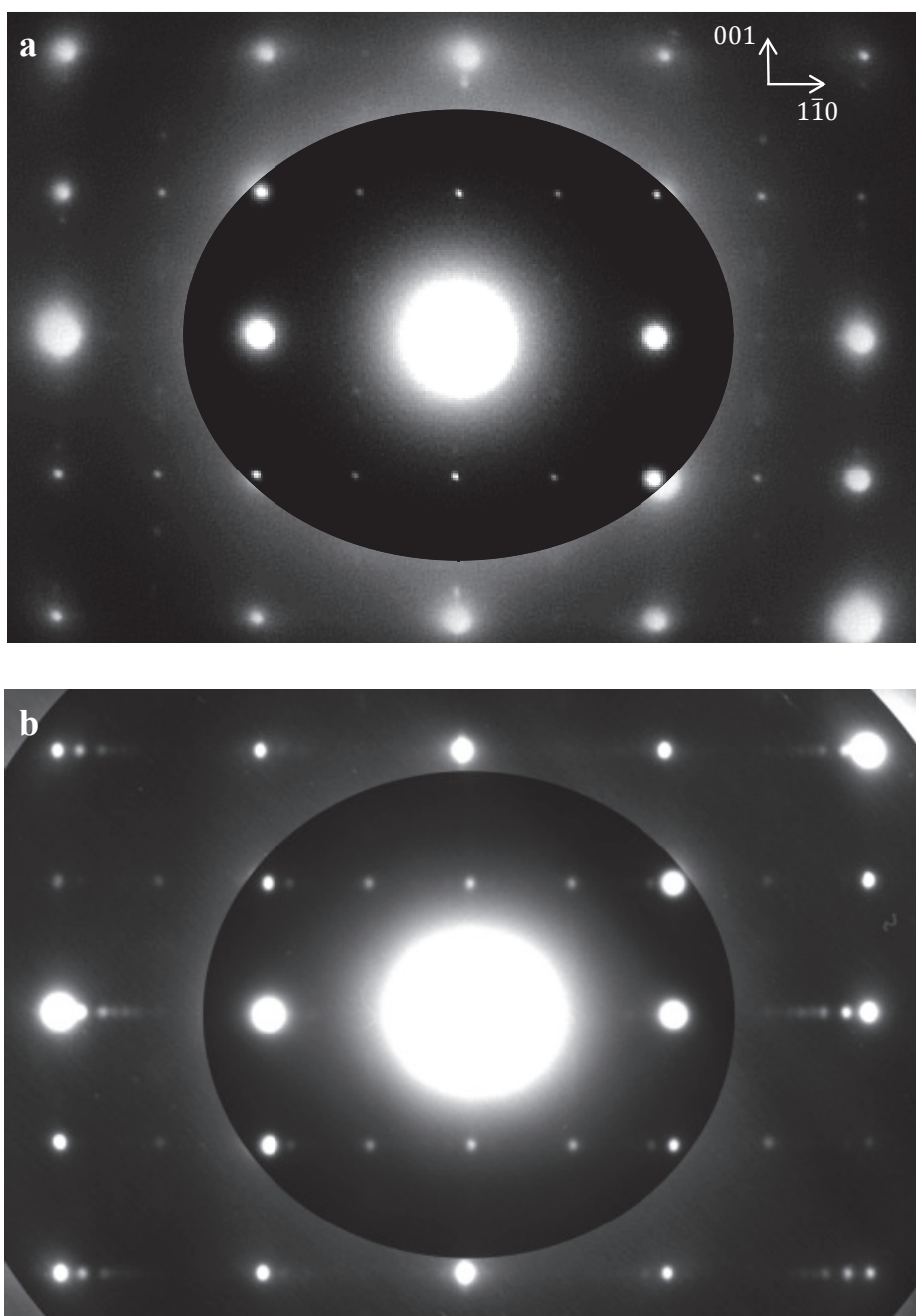
Figure 3.3. Diffraction patterns of air-annealed $SrTiO_3$(110). The same diffraction taken at different exposure times were superimposed to show surface spots close to the direct beam.

(a) After annealing for 5 hours at 1250°C, (5x1) reconstruction was observed. At 1150°C, similar results were obtained with additional streaking in the $[1\bar{1}0]$ direction.

(b) Annealing at 1150°C for 3 hours yielded a coreconstruction of (1x4) and (1x5).
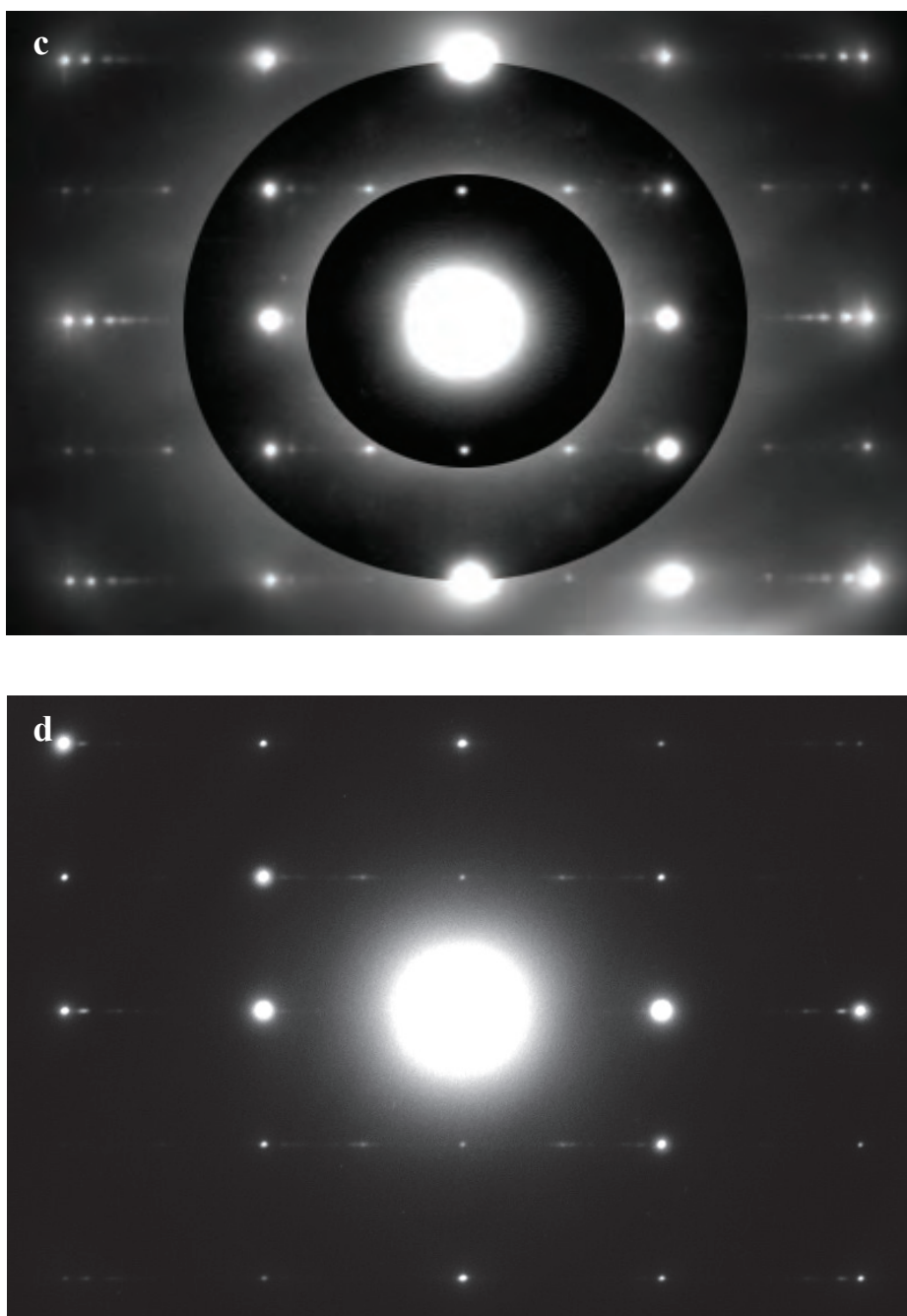
Figure 3.3. (continued) Diffraction patterns of air-annealed SrTiO₃(110).

(c) Annealing for 5 hours at 1050°C resulted in a fully reconstructed (1x5) reconstruction.

(d) Streaking with some not very well-defined diffraction spots were observed in the $[1\bar{1}0]$ direction at 950°C, indicating a partially reconstructed surface.

Summarizing all the observed reconstructions into a time-temperature-transformation diagram (Figure 3.4) based on the detailed data in Table 3.2, it could be said that there seem to be a transition from (1xn) to (nx1) reconstruction at certain time and temperature. At lower temperature and shorter times, (1xn) reconstruction was observed. At higher annealing temperature, (nx1) reconstructions similar to what have been found in the literature were observed. At temperature below 950°C, annealing time does not seem to affect the resulting reconstruction type. At 1150°C, however, it was observed that the (1xn) type reconstructions in samples annealed for less than 3 hours was not as favorable as (nx1) type reconstructions when the annealing time was increased to 5 hours. More experiments are needed to further investigate the trend of reconstructions at varying annealing conditions.

The (3x1) reconstruction on STO (110) observed by Russell and Castell (2008) has been recently solved by Enterkin et al. (2010). Using STM analysis and DFT calculations, it has been found that there are TiO_4 tetrahedra on the surface, and that both charge and bond length increase with increasing depth into the bulk (Enterkin et al., 2010). However, the mechanisms behind (1xn) type reconstruction are still unknown and the reconstructed structure has not been solved. Hence, instead of carrying out more experiments to find out which type of reconstructions occur under what annealing conditions, the next steps of this study focus more on refining the structure using the experimental results.

Table 3.2. Summary of annealing conditions and the corresponding observations in this work.

Time (hours)	Temperature (°C)	Observation
5	875	Streaking in [110]
5; 10*	875	(1x5)
5	950	(1x5)
5; 10*	950	(1x4) or (1x5)
5	1050	(1x5)
1	1150	(1x4)
3	1150	(1x4) and (1x5)
5	1150	(5x1), slight streaking in [110]
5	1250	(5x1)

*Note: These samples were first annealed for 5 hours, and then for another 10 hours.
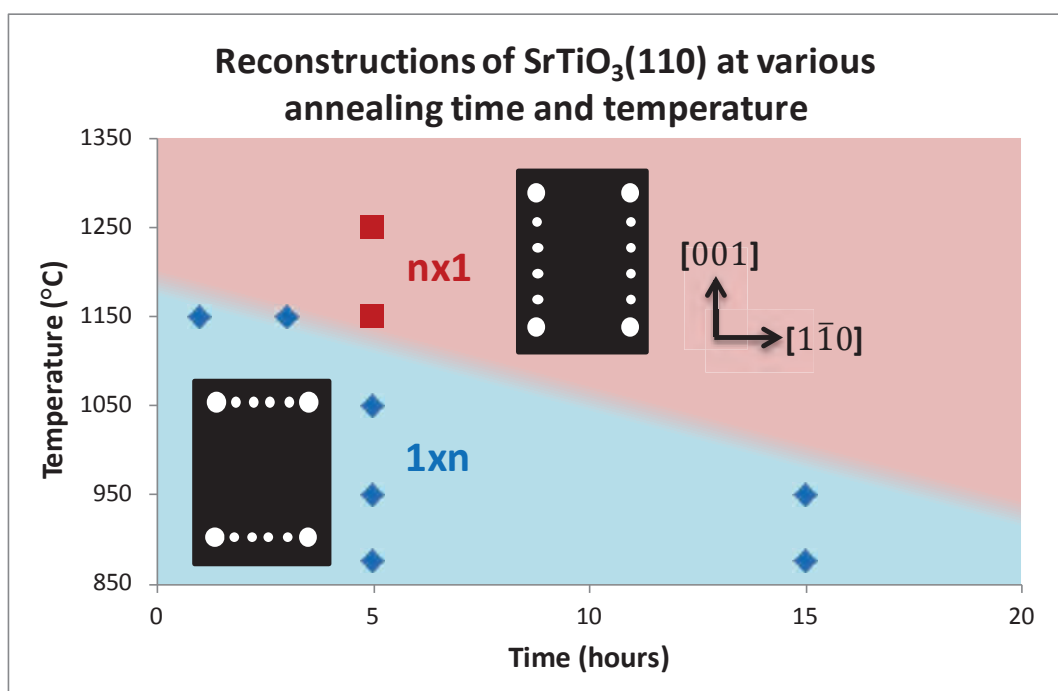
Figure 3.4. Reconstructions of SrTiO$_3$ (110) air-annealed at various time and temperature. Red squares represent the observed (nx1) periodicities and blue diamonds represent (1xn) reconstructions, where n = 4 or 5. Schematic representations of the two reconstruction types are shown. The four big white circles at the corners indicate bulk atoms that form a unit cell for each case, whereas small white circles represent surface atoms on the reconstructed surfaces.

3.4 Electron Direct Methods

Transmission electron diffraction patterns were documented using negative films. Diffraction patterns were taken at different exposure times ranging from 0.5s to 120s. Negative films were developed in the dark room and then digitized with an Optronics P-1000 microdensitometer using the parameters stated in Table 3.3. The .raw files were later opened in the software Electron Direct Methods (EDM) to be analyzed.

In this study, EDM version 3.2 was used to quantify the peak intensities of diffraction patterns showing (1x5) reconstruction. A complete explanation on how the program works is beyond the scope of this work. However, a worked example of using EDM to solve structures using diffraction data is provided below. More detailed explanation and program interface examples can be found on the EDM website (Kilaas et al., 2006).

To quantify diffraction spots, EDM uses a cross-correlation based method and symmetry averaging. First, lattice points were defined on the .raw files. Diffraction peaks were measured and converted to numerical data that will be used by Direct Methods (DM). Symmetrized reflections from each diffraction pattern were saved. The measured intensities were then averaged using a p2mm Patterson symmetry, yielding 63 reflections ready to be used in DM analysis. Since glide plane would not be commensurate with the bulk truncation, the only possible plane group symmetries were *pm* and *p2mm* (Enterkin et al., 2010). Direct methods were used for both plane groups to search for possible solutions.

Table 3.3. Parameters used in digitizing negative films with the Optronics system.

Pixel/line	Lines/band	Pixel offset in mm	Line offset in mm	Raster size in μm	Filter
2000	2000	10	20	25	White

Convergence analysis and genetic analysis were run in Direct Methods. Convergence analysis uses measured amplitude data and selects reflections with phases that are significant in defining phases of other reflections. Genetic analysis uses generic algorithms to alter the values of the phases that the convergence analysis found to be significant, and then finds the most feasible values to generate hundreds of general solutions. A suitable cross correlation difference value is entered to restrict the number of unique solutions for refinement. In general, structures that have lower figure of merit (FOM) or low R and χ^2 values are more possible solutions although this is not always the case. Density functional theory (DFT) calculations and other complimentary techniques should be performed to confirm the final solution.

3.4.1 Using the p2mm plane group

The *p2mm* plane group was first chosen to be run in DM since it has higher order symmetry than the *pm* plane group. The unique solutions found by DM share a general trend of having four strong potentials, possibly titanium atoms, surrounding a weaker one, suggesting a tetrahedral structure. In many cases, only parts of the maps contain visible potential, as seen most obviously in Figure 3.5a. This could arise from the possibility that surface reconstruction is absent in those regions, or that there are light elements that are not well represented in the potential maps. The way DM works is such that strong atom-like features (heavier elements) are reinforced but weaker features (lighter elements) are not (Marks et al., 2001). Hence it is not uncommon that refinement work starts with guessing the locations of heavy elements from the initial potential maps and then fitting lighter elements afterwards (Marks, 2011). The weak periodic background seen in Figure 3.5a, c, and d could also indicate modulation. Modulation is
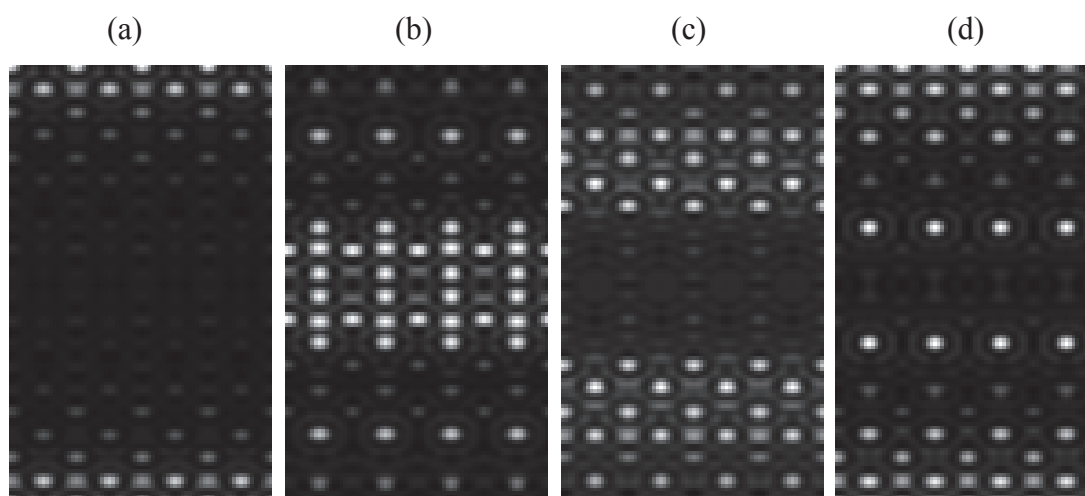
Figure 3.5. Four of the unique solutions found by DM using the *p2mm* symmetry.

similar to a series of dipoles instead of having atomistic features, hence it will not be well represented in DM (Marks, 2011).

Based on the potential maps, several guesses were refined in EDM and the structures that gave low enough R and χ^2 values were considered possible solutions (Marks et al., 2001). Ideally R should be as low as 0.15 and χ^2 should be 2.0 or lower (Marks, 2011). Atomic structure models of the possible solutions were then drawn using the software ATOMS. Density functional theory (DFT) calculations were performed on these models to gauge whether the energies of these models are low enough for the models to be considered stable structures. Conversely, one can first design sensible structures based on knowledge of chemistry, then only subject the models to DFT calculations. If the models are found to have low energies, then the known atomic types and positions can be inputted into Direct Methods to check for the R and χ^2 values of the structures. Figure 3.6a was drawn using the approach whereas Figure 3.6b was created using the second approach. Since Figure 3.6b is a result of DFT calculations, it is not surprising that the structure is relaxed (layers of near-surface atoms deviated from bulk positions) compared to Figure 3.6a.

(a)

Plan view

Side view

(b)

[1̄10]

[001]

[1̄10]

[110]
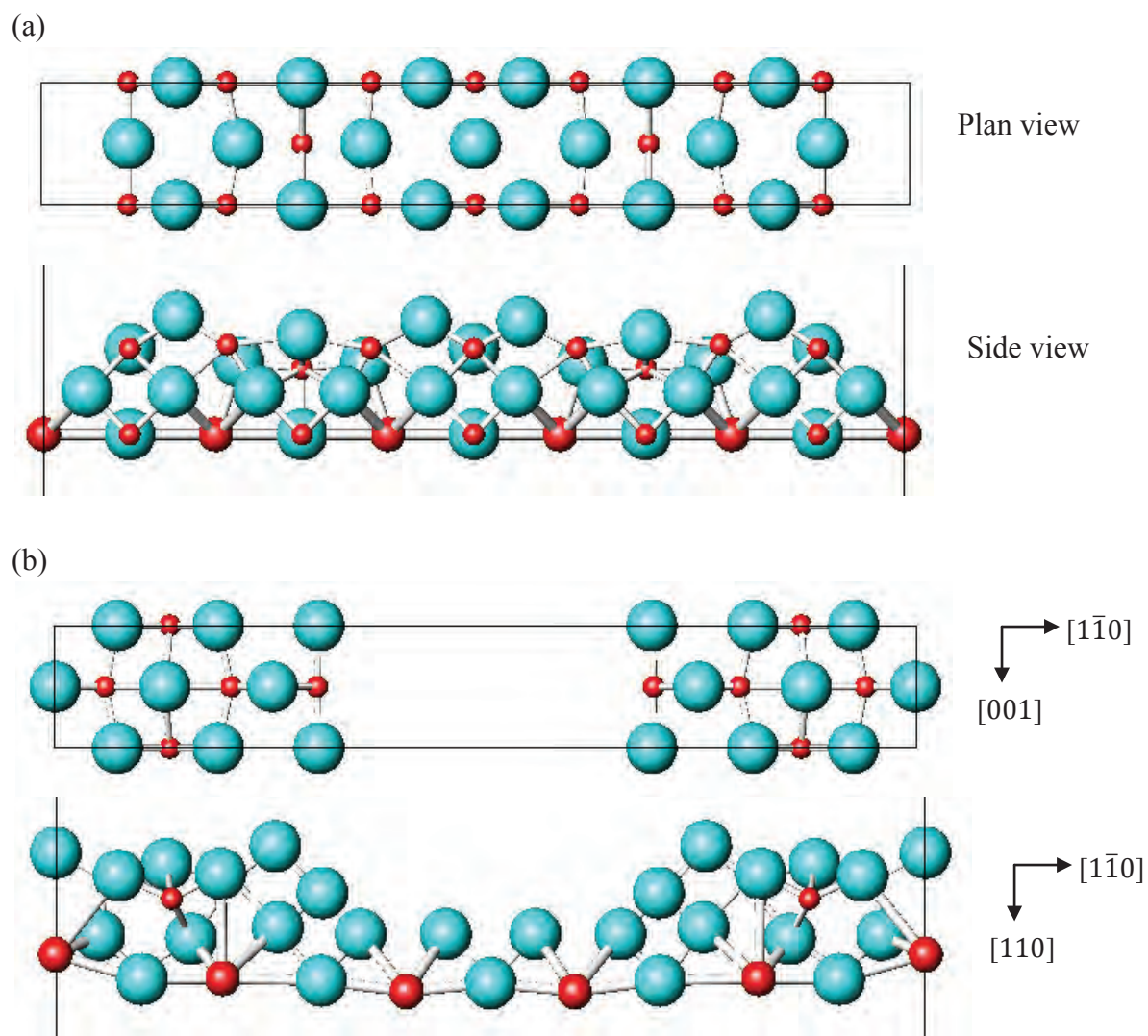
Figure 3.6. Plan view and side view of two possible structures using the p2mm plane group symmetry. Structure (a) has 9 Ti per (1x5) unit cell and was built in ATOMS based on refinements in DM. Structure (b) has 8 Ti per (1x5) unit cell and is a result of DFT calculations, hence the surface structures are relaxed.

Some of the structures have R values of approximately 0.28 and a χ^2 slightly above 2.5 after being refined. Although these structures seem possible in terms of coordination and are valence neutral, DFT calculations showed that they have very high energies and therefore are not energetically favorable. Hence, it is reasonable to turn to *pm* symmetry to look for possible solutions.

3.4.2   Using the pm plane group

The *pm* plane group was run in DM and a set of unique solutions were found. Four of the potential maps are shown in Figure 3.7. A larger region in each potential map appeared to be dark compared to maps generated using the *p2mm* plane group. The general trend of four strong potentials surrounding a weaker one, which was observed in potential maps obtained using the *p2mm* symmetry (Figure 3.6), is also apparent in this case. After refinements were performed in the Peaks program, atomic structures were created using ATOMS.
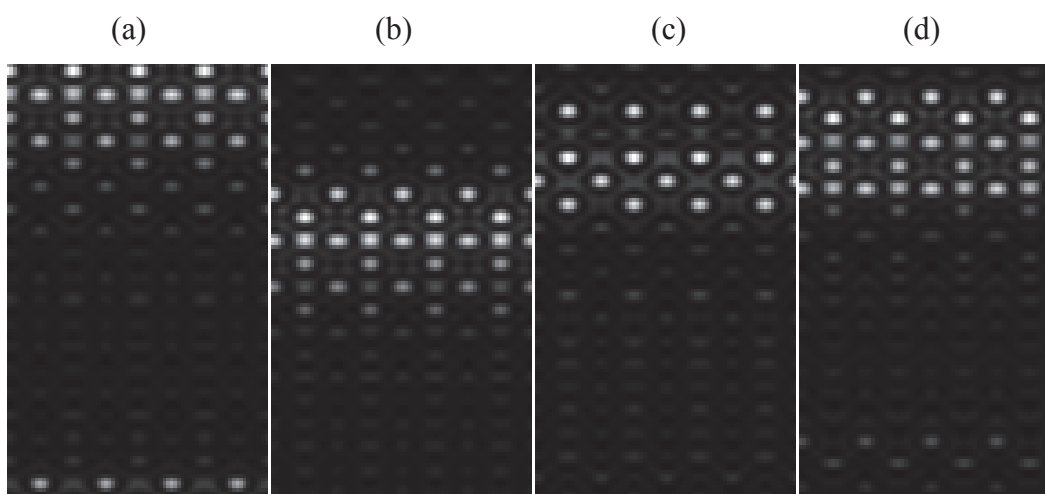

Figure 3.7. Four of the unique solutions found by DM using the *pm* symmetry.

The three structures shown in Figure 3.8 have half of the surface oxygen atoms missing to achieve a valence-neutral stoichiometric surface, and then have one or more TiO_2 units sitting on the surface, forming a hill-like structure. Figure 3.8b is the same as Figure 3.8a except there is an additional layer of TiO_2 units (colored in blue and gold) on the original hill-like structure. Both of these models have energies that seemed favorable from DFT calculations, but the hill-like structures have heights that do not match the STM data (Russell and Castell, 2008) showing (1x4) reconstruction with a height of approximately 1.5 Å. The third structure (Figure 3.8c) was designed to match the height constraint. It has an energy of 2.0 eV per (1x1) unit cell, which is slightly higher than the energy of the previously solved (3x1) structure (Enterkin et al., 2010), and that of the valence-neutral structure with half of the surface oxygen atoms missing (Marks, 2011). The energies of these structures are illustrated in Figure 3.9.

One of the reasons why it is possible to have half of the surface oxygen atoms removed is that some of the oxygen could be terminated with hydrogen when water formed on the surface during sample preparation or annealing treatments since the samples in this study were annealed in ambient air, not UHV or O_2. The water that formed could be removed over the course of high-temperature annealing due to dehydration. Hence, one is left with a valence-neutral surface with half of the oxygen gone, and reconstruction formed on part of that surface.

The structure shown in Figure 3.8c is by far the most promising solution. It matches the potential map, has a height that is close to the STM data, and has a low energy. However, no conclusive results have been found. Currently, more work is being done to confirm the final solution.

(a)

Plan view

Side view

2.5 Å

(b)

[1$\bar{1}$0]

[001]

3.6 Å

[1$\bar{1}$0]

[110]

(c)

1.9 Å
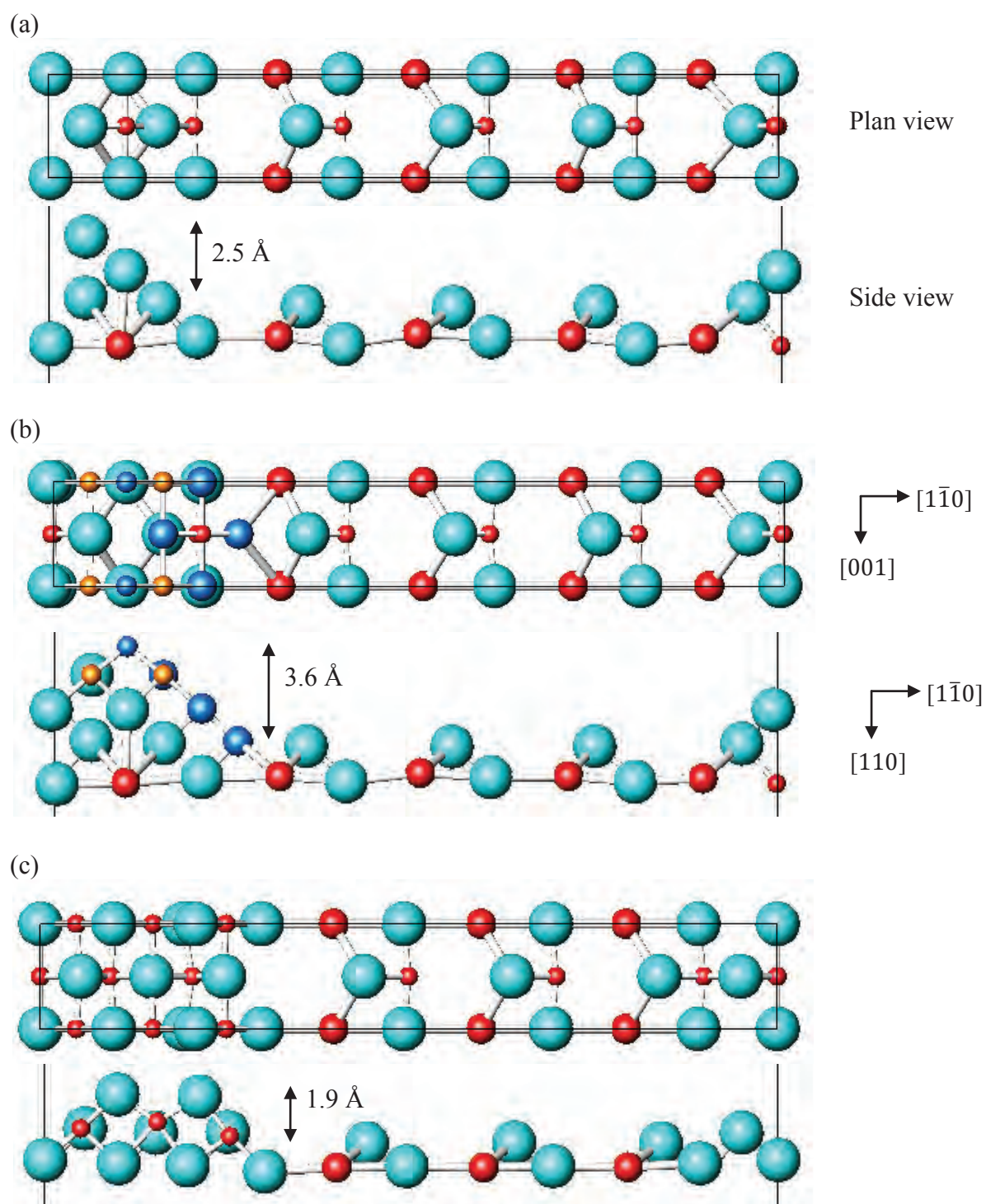
Figure 3.8. Plan view and side view of three possible structures using *pm* symmetry. The estimated height of each surface structure is indicated. Structures (a) and (b) have low energies in DFT calculations whereas (c) matches the height from the STM data.
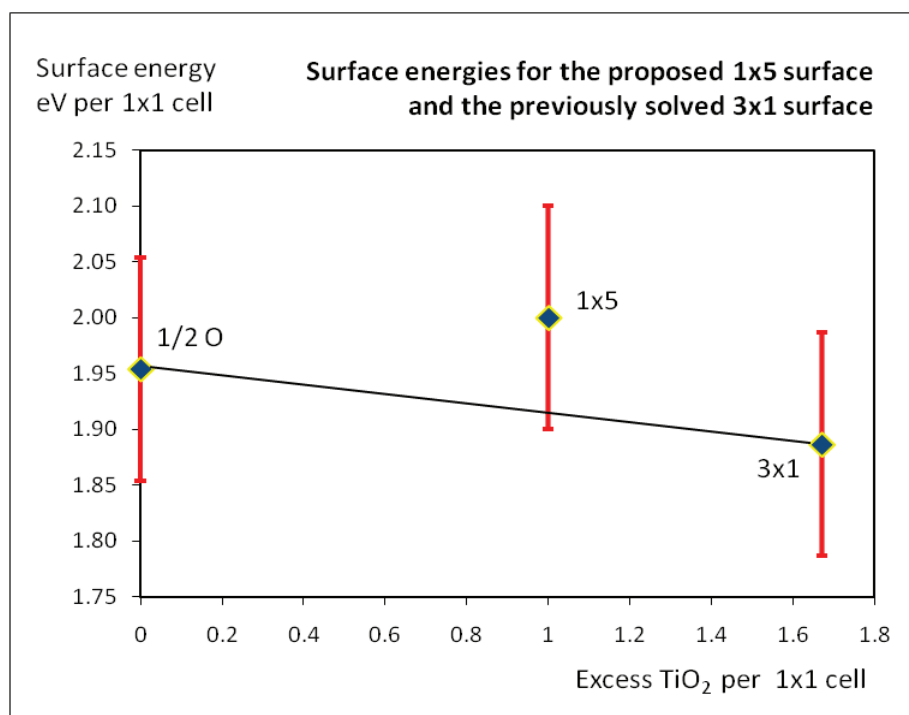
Figure 3.9. Comparison of DFT-calculated surface energies of different models. The proposed (1x5) structure seen in Figure 3.8c has an energy that is slightly higher than both the previously solved (3x1) structure, and the valence-neutral surface structure with half of the oxygen atoms missing.

Chapter 4

Conclusions and Suggestions for Future Work

In this study, it has been found that (1xn) reconstruction occurs at lower annealing temperatures and shorter times whereas (nx1) reconstruction was observed at higher annealing temperatures. The sample annealed at 875°C for 5 hours showed streaking along the $[1\bar{1}0]$ direction, indicating surface reconstruction has started but the surface has not fully reconstructed. The 950°C anneal also showed streaking along the $[1\bar{1}0]$ direction but some discrete diffraction spots can be observed. In the 1050°C anneal, the surface has fully reconstructed. Evenly spaced surface diffraction spots along the $[1\bar{1}0]$ direction were observed, indicating (1x5) reconstruction. At 1150°C, the sample showed a combination of (1x4) and (1x5) reconstructions when annealed for 3 hours, but (5x1) reconstruction with streaking along $[1\bar{1}0]$ was observed when the sample was annealed for 5 hours. The sample annealed at 1250°C for 5 hours no longer show reconstructions along the $[1\bar{1}0]$ direction but surface diffraction spots along the [001] direction were observed, indicating (3x1) or (4x1) reconstruction that was observed in previous studies. To further investigate the trend of reconstruction type as a function of annealing time and temperature, more experiments have to be carried out.

The (1xn) reconstructions were not observed as a primary or dominant reconstruction type in previous work. Electron Direct Methods were used to recover phase information lost in electron diffraction to make a good estimate of an initial structure for further refinement. The solution has to fulfill three constraints: (i) yield a low R and a low χ^2 value in the Peaks

refinement code; (ii) have a low energy in DFT calculations; (iii) have a height that matches the STM data obtained by Russell and Castell (2008).

Much effort has zeroed in on find *the* solution that matches all three constraints mentioned above. There is a set of possible solutions that match either only one or two constraints. Currently there is one solution that fulfills all constraints and seems very promising. However, more calculations and refinements need to be done to confirm the final solution. Since there is very limited experimental data to support or provide more clues in solving the structure, more analysis has to be done on the BF/DF images in hope of extracting information that can help solve the structure. The specimens can be viewed under the TEM to obtain HREM images, although it is likely that the samples have undergone changes over time.

In the future, more studies can be done on annealing the samples in different environments, such as under ambient air, H_2, O_2 or N_2, since experimental work using these conditions is either very few or none at all. Annealing in UHV but over a different range of temperature could be performed too. Images including BF, DF, and HREM should be recorded with care since they could provide a wealth of information complementing diffraction data.

References

Attfield, J.P. (2001). Structure-property relations in doped perovskite oxides. *International Journal of Inorganic Materials, 3,* 1147-1152.

Bachelet, R., Valle, F., Infante, I. C., Sanchez, F., &Fontcuberta, J. (2007). Step formation, faceting, and bunching in atomically flat SrTiO$_3$(110) surfaces. *Applied Physics Letters, 91*, 251904.

Bando, H., Aiura, Y., Haruyama, Y., Shimizu, T., & Nishihara, Y. (1995). Structure and electronic states on reduced SrTiO$_3$(110) surface observed by scanning tunneling microscopy and spectroscopy. *Journal of Vacuum Science and Technology B, 13*(3), 1150-1154.

Bendersky, L. A., & Gayle, F. W. (2001).Electron diffraction using transmission electron microscopy.*Journal of Research of the National Institute of Standards and Technology, 106(6)*, 997-1012.

Bhasin, M. M., (1999). Importance of surface science and fundamental studies in heterogeneous catalysis. *Catalysis Letters, 59*, 1-7.

Biswas, A., Rossen, P. B., Yang, C. H., Siemons, W., Jung, M. H., Yang, I. K., Ramesh, R., and Jeong, Y. H. (2011). Universal Ti-rich termination of atomically flat SrTiO$_3$ (001), (110), and (111) surfaces. *Applied Physics Letter, 98,* 051904.

Brasunas, J.C., Cushman, G. M., Lakew, B. (1999). Thickness measurement. *CRC Press LLC.*

Brunen, J., Zegenhagen, J. (1997). Investigation of the SrTiO$_3$ (110) surface by means of LEED, scanning electron tunneling microscopy and Auger spectroscopy. *Surface Science, 389,* 349-365.

Castell, M. R. (2002). Scanning tunneling microscopy on reconstructions on the SrTiO$_3$ (001) surface. *Surface Science, 505*, 1-13.

Chiaramonti, A. N. (2005). *Structure and thermodynamics of model catalytic oxide surfaces.* Ph.D. Thesis. Northwestern University, Illinois, United States.

Chiaramonti, A. N., Lanier, C. H., Marks, L. D., & Stair, P. C. (2008). Time, temperature, and oxygen partial pressure-dependent surface reconstructions on SrTiO$_3$ (111): A systemic study of oxygen-rich conditions. *Surface Science, 602,* 3018-3025.

Copie, O., Garcia, V., Bodefeld, C., Carretero, C., Bibes, M., Herranz, G., Jacquet, E., Maurice, J. L., Vinter, B., Fusil, S., Bouzehouane, K., Jaffres, H., and Barthelemy, A. (2009). Towards two-dimensional metallic behavior at LaAlO$_3$/SrTiO$_3$ interfaces. *Physical Review Letters, 102,* 216804.

Deak, D. S. (2007). Strontium titanate surfaces. *Materials Science and Technology*, *23*, 127-136.

Enterkin, J. (2009). Private Communication.

Enterkin, J. A., Subramanian, A. K., Russell, B. C., Castell, M. R., Poeppelmeier, K. R., & Marks, L. D. (2010). A homologous series of structures on the surface of SrTiO$_3$ (110). *Nature Materials, 9,* 245-248.

Erdman, N., Poeppelmeier, K.R., Asta, M., Warschkow, O., Ellis, D.E., and Marks, L.D. (2002). The structure and chemistry of the TiO$_2$-rich surface of SrTiO$_3$ (001). *Nature, 419,* 55-58.

Gunhold, A., Gomann, K., Beuermann, L., Kempter, V., Borchardt, G., &Maus-Friedrichs, W. (2004). Changes in the surface topography and electronic structure of SrTiO$_3$ (110) single crystal heated under oxidizing and reducing conditions. *Surface Science, 566-568,* 105-110.

Huang, Y.H., Zhao, K., Lu, H. B., He, M., Jin, K. J., Chen, Z. H., Zhou, Y. L., and Yang, G. Z. (2007). Ultraviolet photoresponse properties of SrTiO$_3$ single crystals. *The European Physical Journal Applied Physics, 38,* 37-39.

Huijben, M., Brinkman, A., Koster, G., Rijnders, G., Hilgenkamp, H., and Blank, D. H.A. (2009). Structure-property relation of SrTiO$_3$/LaAlO$_3$ interfaces. *Advanced Materials, 21,* 1665-1677.

Kilaas, R., Own, C., Deng, B., Tsuda, K., Sinkler, W., & Marks, L. (2006). EDM: Electron Direct Methods Release 2.0.1, June 2006. www.numis.northwestern.edu/edm/documentation/edm.htm

Klauber, C., Smart, R. S. C., (2003). Solid surfaces, their structure and composition: Importance of the surface. In O'Connor, D. J., Sexton, B. A., Smart, R. C. (Eds.), *Surface analysis method in Materials Science* (pp. 3-6). Berlin, Germany: Springer-Verlag.

Lanier, C. H. (2007). *Oxide surfaces in practical and model catalytic systems.* Ph.D. Thesis. Northwestern University, Illinois, United States.

Marks, L.D. (1996). Wiener-filter enhancement of noisy HREM images. *Ultramicroscopy, 62,* 43-52.

Marks, L.D. (2011). Private communication.

Marks, L.D., Chiaramonti, A. N., Tran, F., Blaha, P. (2009). The small unit cell reconstructions of $SrTiO_3$(111). Surface Science, doi:10.1016/j.susc.2009.04.016

Marks, L.D., Erdman, N., and Subramanian, A. (2001). Cryatallographic direct methods for surfaces. *Journal of Physics: Condensed Matter, 13,* 10677-10688.

Noguera, C. (2000). Polar oxide surfaces. *Journal of Physics: Condensed Matter, 12,* R367-R410.

Oura, K., Lifshits, V.G., Saranin, A.A., Zotov, A.V., and Katayama, M. (2003) *Surface Science: An Introduction.* Berlin: Springer-Verlag.
Own, C. (2005). *System design and verification of the precession electron diffraction technique.* Ph.D. Thesis. Northwestern University, Illinois, United States.

Russell, B. C., & Castell, M. R. (2008). Reconstructions on the polar $SrTiO_3$ (110) surface: Analysis using STM, LEED and AES. *Physical Review B, 77,* 245414.

Subramanian, A., and Marks, L.D. (2004). Surface crystallography via electron microscopy. *Ultramicroscopy, 98,* 151-157.

Venables, J., Smith, D. J., and Cowley, J. M. (1987). HREM, STEM, REM, SEM and STM. *Surface Science, 181,* 235-249.